HUNTINGTON MEDICAL RESEARCH INSTITUTES
NEURAL ENGINEERING PROGRAM
734 Fairmount Avenue
Pasadena, California 91105

Contract No. N01-NS-1-2340
Quarterly Progress Report
July1- Sept 30, 2002
Report No.4

"Functional Microstimulation of the Lumbosacral Spinal Cord"

Douglas McCreery, Ph. D.
Albert Lossinsky, Ph.D.
Victor Pikov, Ph.D
Leo Bullara, B.A.
William Agnew, Ph.D.

ABSTRACT

The objective of this project is to develop neuroprostheses that will allow patients with severe spinal cord injuries to regain control of their bladder and bowel. The approach is based on an array of microelectrodes that is implanted into the sacral spinal cord. During the past quarter, an array of 9 discrete iridium microelectrodes was implanted into the sacral spinal cords of cats SP135,SP137 and SP138. The tips of these electrodes were slightly sharper (radius of curvature of 2-3 ：m vs 5-6 ：m in previous animals) to determine if this would affect the gliotic scarring that frequently occurs ventral to the tips sites. A silicon-substrate array with 6 shanks and 12 electrode sites was implanted into the caudal S_1 spinal cord of cat SP136.

During the previous quarter, cat SP134 had been implanted with an array of 9 iridium electrodes. Urodynamic measurements were obtained from this animal at 40 and at 88 days after implanting the arrays. At both post-implant times, an elevation in bladder pressure greater than 35 mm Hg and also relaxation of the urethral sphincter could be elicited by pulsing with selected electrodes. Two of the electrodes elicited weak but continuous micturition.

The silicon array implanted into cat SP136 continued to function throughout the full 57 days *in vivo.* At 14 and also at 57 days after implantation, an increase in bladder pressure greater than 40 mm Hg could be elicited from at least two of the electrodes. The histologic evaluation of the implant site revealed no evidence of old or recent hemorrhages near any of the 6 silicon shanks. The lateral shanks were surrounded by a sheath of connective tissue that was somewhat thicker (approximately 25 ：m) than is typical of the discrete iridium shafts, but along most of the length of the shafts, there were viable neurons within 100 ：m of the track. As in the previous cat chronically implanted with a silicon-substrate array (SP131) there was a noticeable reduction in the density of NeuN-positive neurons around the tips of all 6 shanks. In contrast to the lateral shanks, there was considerable tissue damage around these medials shanks (Figures 14A,14B). Clearly, the silicon-substrate array must be modified so that the neurons of the central gray commissure can be stimulated, without damaging this region.

In cat SP135, the radius of curvature of the electrode tips varied from 2.3 to 4.5 ：m. A persisting problem with these implants in the feline sacral spinal cord has been the occurrence of glia scars ventral to the electrode tips sites In cat SP135, there was no discernable difference in the severity of the scarring produced by the blunt and the sharp electrodes.

METHODS

The objective of this project is to develop neural prostheses that will allow patients with severe spinal cord injuries to regain control of their bladder and bowel. The system is based on an array of microelectrodes that is implanted into the sacral spinal cord. The procedures and hardware are being developed in cats with intact spinal cords, and in the 2nd year of the project, the implanted cats will undergo transection of the spinal cord at the low thoracic level.

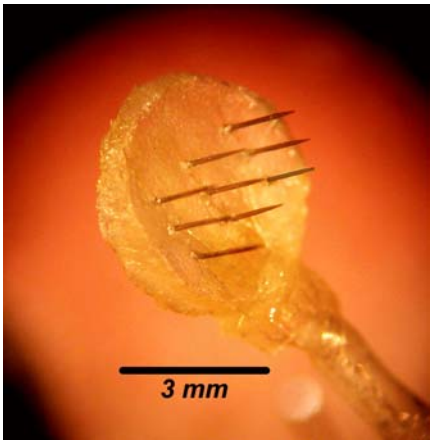

Figure 1

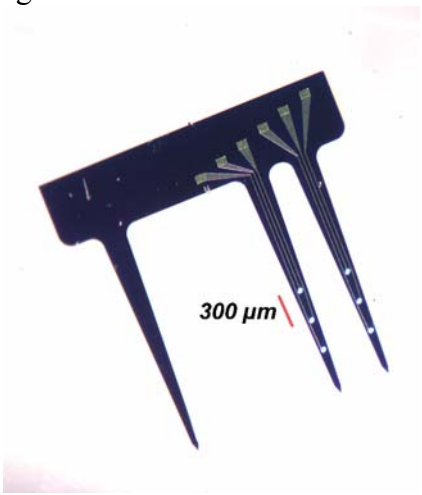

Figure 2A

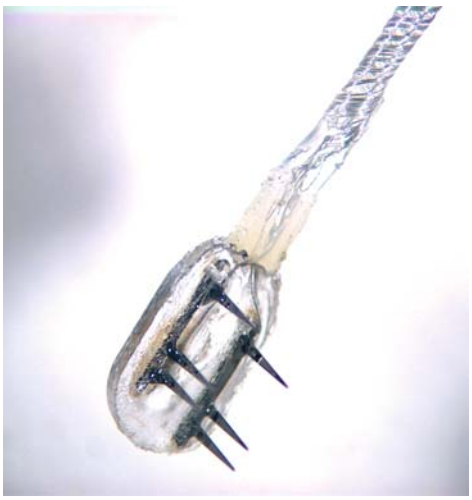
Figure 2B

Fabrication and implantation of the microelectrode arrays

Discrete iridium microelectrodes with exposed surface areas of approximately 2,000 : m^2 were fabricated as described previously. The arrays of 9 iridium microelectrodes extend from an epoxy superstructure (Figure 1). The 3 microelectrodes comprising the middle row are 1.4 mm in length. In cats SP134 and SP135, the electrodes in the outboard rows were 1.5 mm in length, while in cats SP137 and SP138, they were 1.8 mm in length. The middle and outboard rows were separated by 0.8 mm, and the electrodes in each row (rostral-caudal separation) was 0.5 mm.

The sacral cord is exposed using a standard dorsal laminectomy. To locate the junction of the S_1 and S_2 segments, we stimulate the perigenital skin, which is innervated from the S_2 dorsal root, and record at intervals of 2 mm along the rostral-caudal dimension on the dorsal surface of the sacral cord. The arrays were implanted near the maximum of the 2nd component of the evoked response (the dorsal cord potential). At autopsy, the position of the array was validated by complete dissection of the spinal roots.

Our contract's work scope also includes the development of a 16-site microstimulation array based on multisite silicon substrate probes. Figure 2A shows a probe that was designed for our program by Jamile Hetke at the University of Michigan. Figure 2B shows a completed array containing two probes (total of 12 electrodes sites) extending from an epoxy superstructure. One array was implanted into the sacral cord of cat SP136.

All of the arrays were inserted with the high-speed inserter tool, at a velocity of approximately 1 m/sec. The dura was then closed over the array, using 5 to 7 pre-installed sutures.

Urodynamic measurements of hydrostatic bladder pressure and infusion pressure within the EUS were obtained at intervals after implantation. During this procedure, the cats were anesthetized lightly with Propofol. The apparatus used for these measurements has been described previously (QPR

#1, #2). In all cases, the stimulus was charge-balanced, cathodic-first pulses, 400 ：s/phase in duration, and 100 ：A in amplitude, at 20 pulses per second.

Histologic Procedures

The cats were deeply anesthetized with pentobarbital, given i.v. heparin and perfused through the aorta for 30 seconds with a prewash solution consisting of phosphate-buffered saline, and 0.05% procaine HCl. This was followed by a fixative containing 4% formalin prepared freshly from paraformaldehyde in 0.1 M sodium phosphate buffer. Tissue blocks containing both the microelectrodes and areas rostral and caudal to the electrodes were washed overnight in 4% formalin, then in distilled water for 2 hrs, dehydrated in a graded series of ethanol and embedded in paraffin. The paraffin-embedded tissue blocks were cut at a thickness of 6-7 ：m and were picked up on histogrip-coated-slides (4 sections per slide). These slides were routed either for routine histologic staining with cresyl violet (Nissl), or for immunohistochemistry (NeuN).

Electrode tips were located in unstained sections. The group of slides containing the electrode tips were stained for the neuron-specific protein NeuN, with cresyl violet counterstain or with cresyl violet alone, in an alternating pattern. This allowed each electrode tip to be evaluated using both stains. Histologic sections were photographed using a SPOT Insight digital microscope camera with 1600 x 1200 pixel resolution.

RESULTS

Cat SP134 The effects of the intraspinal microstimulation on the hydrostatic pressure within the bladder and the infusion pressure within the urethral sphincter were measured at 40 and 88 days after implantation of the array. Electrodes 4, 5 & 6 were open-circuited this time, probably due to improper soldering technique by the trainee-technician. At 40 days after implantation, stimulating with electrodes 1, 2, 3, 7, 8 and 9 induced an increase in bladder pressure of 35 mm Hg or more, and these electrodes also induced relaxation of the urethra sphincter. Electrodes 7, 8 & 9 comprise the middle row of electrodes, and normally, would not be expected to induce an increase in bladder pressure. However, the middle and outboard rows of electrodes are separated only by 0.8 mm, so if the array is mis-centered during implantation by as little as 0.4 mm, the medial and one of the outboard rows will be in the intermediate horn, in a location from which both relaxation of the sphincter and elevation of bladder pressure may be elicited. Electrodes #7 & 8 produce weak but steady micturition after the catheter was removed from the urethra.

By 88 days after implantation, the microstimulation was at least as effective as at 40 days. Again, electrodes 7 & 9 produced a large sustained increase in bladder pressure although electrode 8 was now less effective. Electrodes 1-9 all produced a marked decrease in the tone of the urethral sphincter. Figures 3A & 3B show the effect of electrode 9. Stimulation with

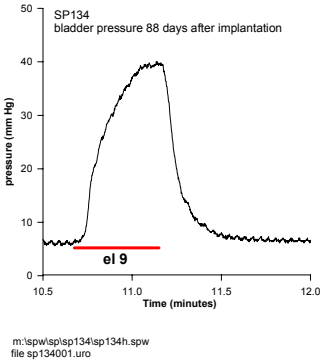

Figure 3A

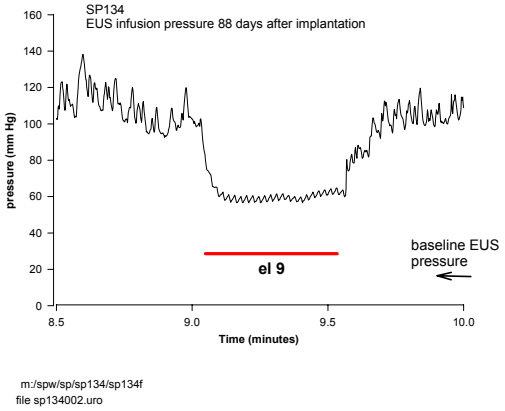

Figure 3B

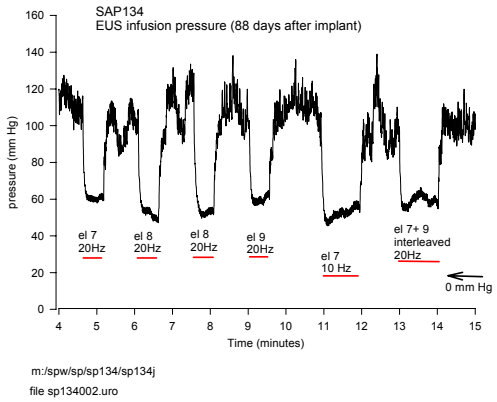

Figure 4

electrodes 7 and 9 (but not with electrode 8) induced weak but steady micturition. Figure 4 shows the relaxation of the urethra sphincter induced by electrodes 7, 8 or 9. Stimulation (with electrode 7) at 10 Hz produced slightly more relaxation of the sphincter than did stimulation 20 pulses per second. However, stimulating at 20 Hz usually produces a greater increase in bladder pressure, so it probably would be advantageous to induce contraction of the bladder and relaxation of the sphincter via different electrodes, each pulsed at the optimal rate. Figure 4 also shows that interleaved pulsing of 2 electrodes (in this case, #7 & 9) did not produce greater relaxation of the sphincter than when either channel was pulsed individually.

When the baseline pressure within the bladder is set at or above approximately 30 mm

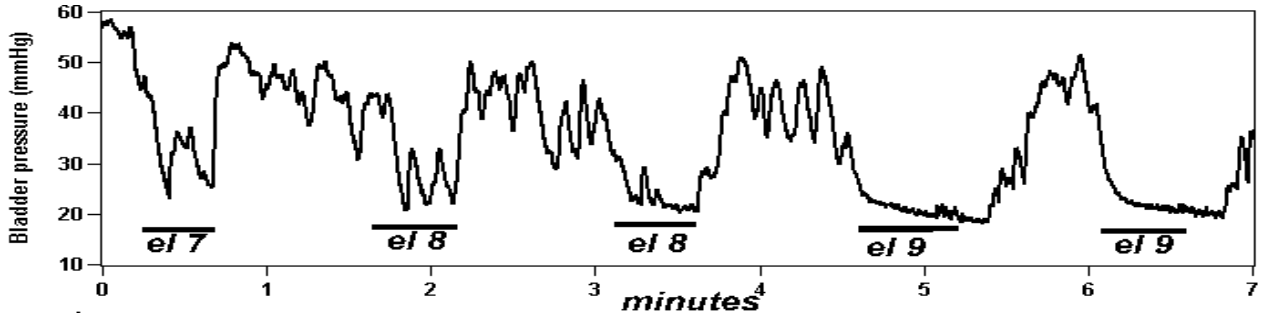

Figure 5

Hg, the bladder soon begins to undergo spontaneous contractions, and if the intraurethral catheter is withdrawn, the cat will urinate. Under these conditions, the intraspinal microstimulation may suppress the spontaneous contractions. The suppression may be elicited from the same sites which induce an elevation of bladder pressure when the baseline pressure is lower, as illustrated in Figure 5. The stimulus parameters were the same as those that induced an elevation of bladder pressure from a lower baseline, when there were no spontaneous contractions (cathodic-first pulse pairs, 100 :A, 400 :s/phase, at 20 Hz).

The urological responses from cat SP134 have been stable for 88 days, and this satisfies our criteria for performing the low thoracic spinal transection. At present, this cat is being treated for an eye infection secondary to a combat-related injury. When he has recovered, the spinal transection will be performed.

Cat SP-136. This cat was implanted with an array of silicon substrate electrodes (Figure 2). At autopsy (Figure 6), the array was determined to be in caudal S_1. Urodynamic measurements were obtained at 14 and at 57 days after implantation of the array. On both dates, electrodes 2 & 5 induced an increase in bladder pressure of more than 40 mm Hg (Figure 7 & 8). Electrodes sites 2 & 5 were closest to the dorsal surface of the cord and, in fact, were close to the lateral margin of the dorsal horn, some distance dorsal to the sacral parasympathetic nucleus (Figures 12A, 13A). However, the dendrites of the sacral parasympathetic nucleus traverse this region (Nadelhaft et al 1980), and it is possible that these dendrites were being stimulated. Figure 6 illustrates another feature of the intraspinal

Figure 6

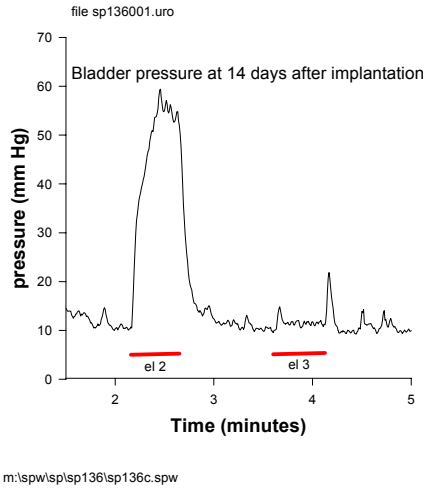

Figure 7

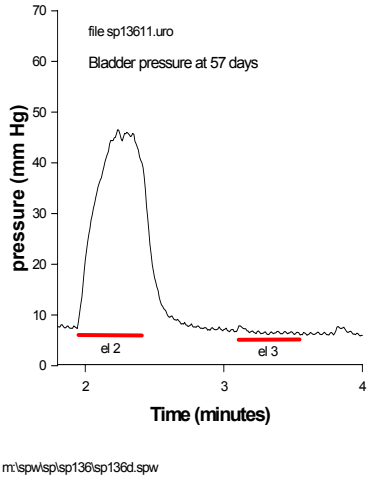

Figure 8

microstimulation that we have reported previously; namely, the high degree of spatial specificity of the stimulation, in spite of the relatively high stimulus amplitude (40 nC/ph). At 14 and at 57 days after implantation, electrode 2 elicited a large increase in bladder pressure while electrode 3, which was only 300 ：m ventral of electrode 2, was ineffective.

None of the electrodes in cat SP136 induced relaxation of the urethral sphincter, and thus none was able to induce micturition. For this reason, the cat was sacrificed at 59 days after implantation, for histologic evaluation of the electrode sites, rather than undergoing a spinal transection. However, the data from this animal clearly illustrates the value of the multisite silicon substrate array for chronic intraspinal microstimulation. Also, the high spatial specificity of the stimulation demonstrates the value of an electrode system with many independent sites.

It is not clear why none of the electrodes was able to induce relaxation of the urethral sphincter, since two of the shanks, each with 3 electrodes, were close to the cord's midline and the dorsal gray commissure. However, there was considerable tissue damage around these medial shanks (Figures 14A, 14B). In contrast, the shanks that had passed though the lateral part of the cord inflicted relatively little damage. Due to the vulnerability of the region around the central canal to injury, it has been our policy to avoid placing microelectrodes into the immediate the vicinity of the central canal, as accidently occurred here. Clearly, the silicon-substrate array must be modified so that the neurons of the central gray commissure can be stimulated, without damaging this region. One solution will be to widen the separation between the two outboard probes and add a medial probe with shorter shanks with will not extend deeper than the central canal (e.g, with shanks approximately 1.5 mm in length)

Cat SP135. This cat was implanted with an array of 9 iridium microelectrodes. All 9 channels failed shortly after implantation, apparently due the weld and solder junctions having been performed at a temperature that was too low to reliably melt the Parylene insulation. The cat was sacrificed 44 days after implantation of the array for histologic evaluation of the implant sites. In this cat, the radius of curvature of the electrode tips varied from 2.3 to 4.5 ：m. A persisting problem with these implants in the feline sacral spinal cord has been the occurrence of glia scars ventral to the electrode tips sites (Figures 9-11). We have not observed this type of injury in the cerebral cortex, the cochlear nucleus or for that matter, in the lumbar enlargement of the cat spinal cord. In cat SP135, there was no discernable difference in the severity of the scarring produced by the blunt (Figure 9) and the sharp electrodes (Figures 10 and 11). In the future, we will use the blunt electrodes, since this will yield a more uniform distribution of current over the exposed electrode tip. The scars tend to be asymmetric and tend to be centered slightly medial to the axis of the electrode. It now seems likely that the tissue damage occurs during the insertion process when the sacral cord is momentarily flattened by the array's epoxy superstructure. In future cats, we will attempt to insert the array in a two-step process, with a rapid (1m/sec) phase to allow the electrodes to penetrate though the pia, followed by slow insertion of the electrodes to their final depth, while compressing the cord as little as possible.

Cat SP137 and SP138 were implanted with arrays of 9 iridium microelectrodes. In these cats,

the outboard microelectrodes were longer (1.8 mm), in order to determine the feasibility of exciting the axons of the preganglionic parasympathetic neurons of the SPN. These axons form a narrow stria along the lateral margin of the ventral horn (Nadelhaft et al, 1980). We would expect that the threshold of the axons would be lower than that of the cell bodies and dendrites. However, in neither of these cats were we able to elicit a large increase in bladder pressure, although some of the medial electrodes did induce relaxation of the urethral sphincter. To date, we have had the most success with electrodes that are 1-4 - 1.5 mm in length.

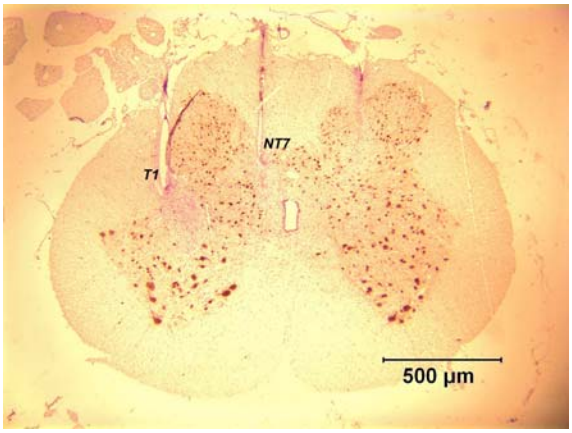

Figure 9A. SP135. Section through the tip site of a blunt microelectrode (e1 with tip radius = 4.5 ：m) and near the tip site of a sharper microelectrode (e7 with tip radius = 3.2 ：m). NeuN + Nissl counterstain.

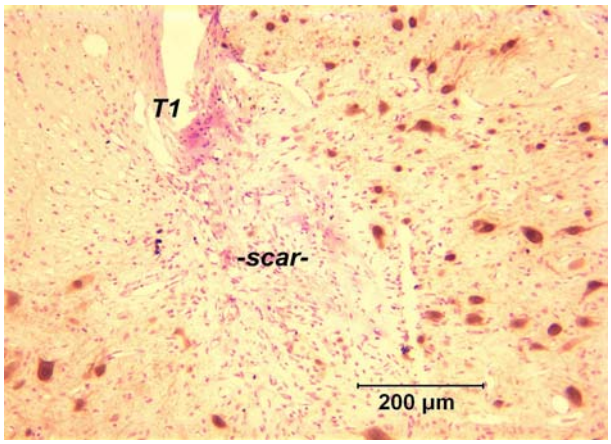

Figure 9B. SP135. Tip site of blunt microelectrode e1, with a large glial scar ventral and medial to the tip site. Note the absence of the brown, NeuN-positive neurons within the scar. NeuN + Nissl counterstain.

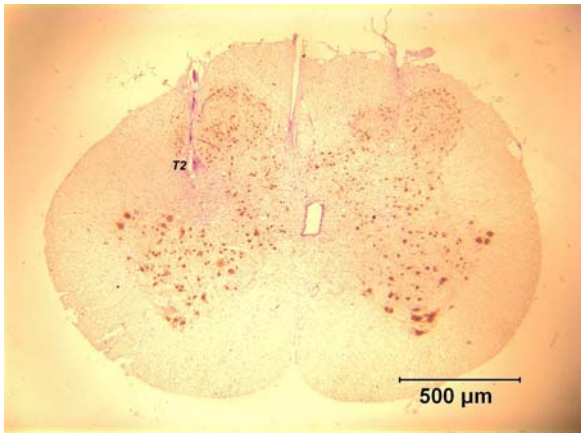

Figure 10A. SP135. Tip site of sharp microelectrode e2 (tip radius = 2.3 ：m). NeuN + Nissl counterstain.

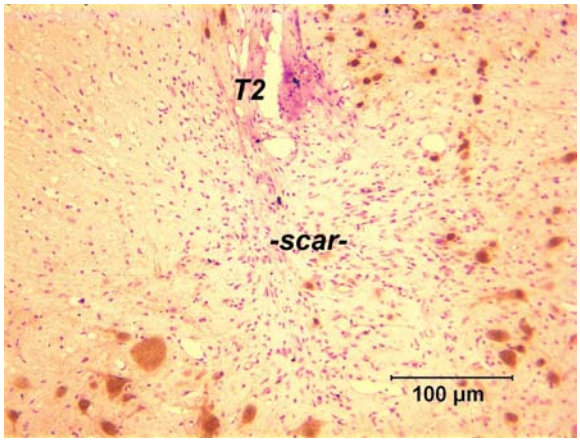

Figure 10B.SP135. Tip site of sharp microelectrode e2, with a 250 ：m diameter glial scar ventral to the tips site. NeuN + Nissl counterstain.

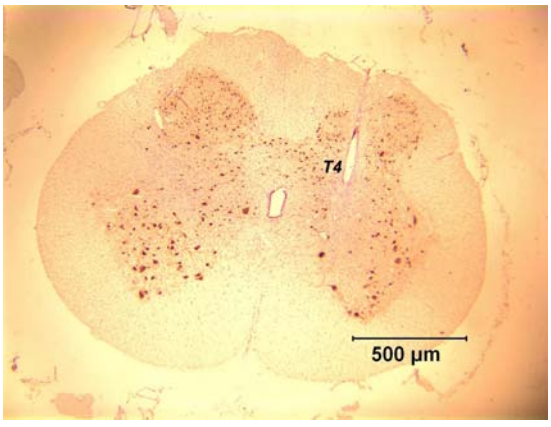

Figure 11A. Tip site of sharp microelectrode e4 (Tip radius = 3.1 ：m) NeuN + Nissl counterstain.

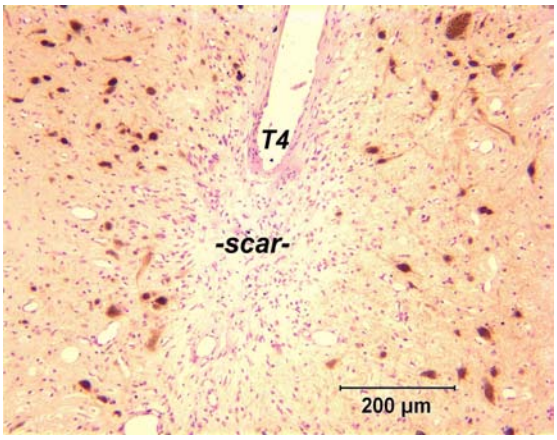

Figure 11B. The tip site of sharp microelectrode e4, with the associated glia scar. NeuN + Nissl counterstain.

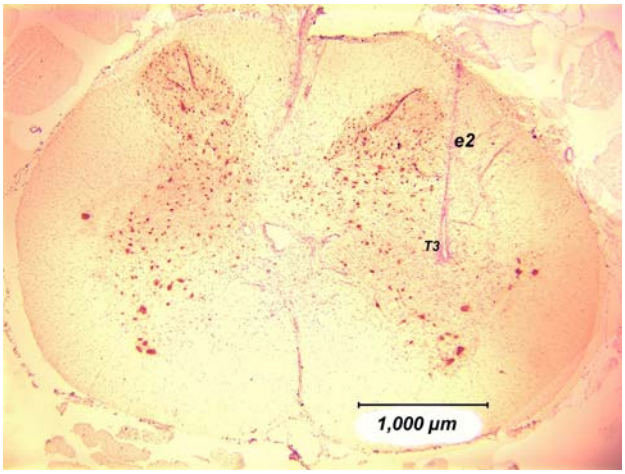

Figure 12A. Sp 136. The track of silicon shank T3. The approximate location of electrode e2 is indicated. NeuN + Nissl counterstain.

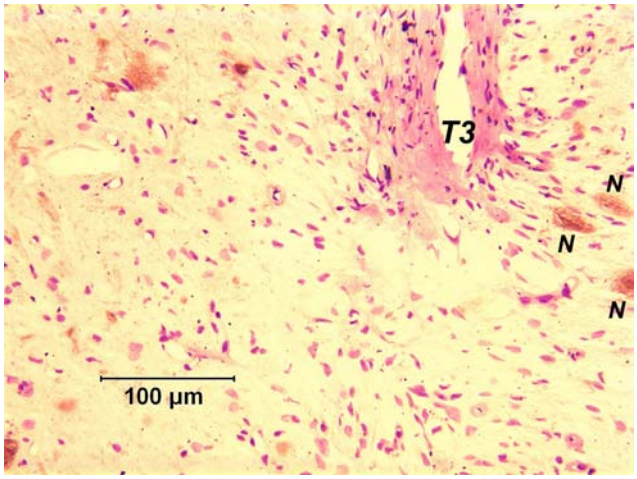

Figure 12B. Higher magnification of the site of the tip of shank T3. The is a reduction in the NeuN-positive neurons near the track, but viable neurons are seen within 100 ：m of the tip. NeuN + Nissl counterstain.

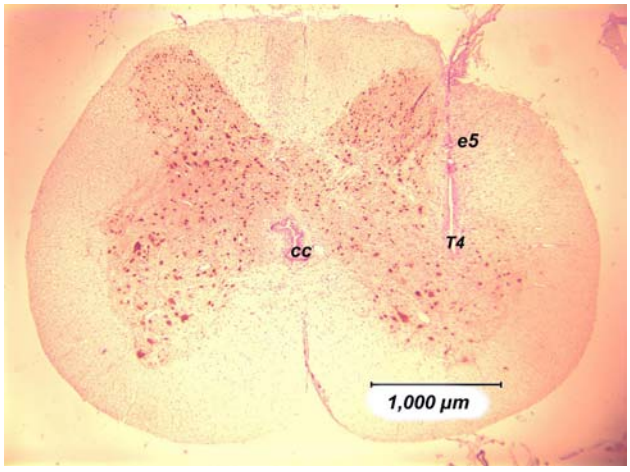

Figure 13. The track of shank T4. The approximate location of electrode 5 on the side of the shank is indicated. NeuN + Nissl counterstain.

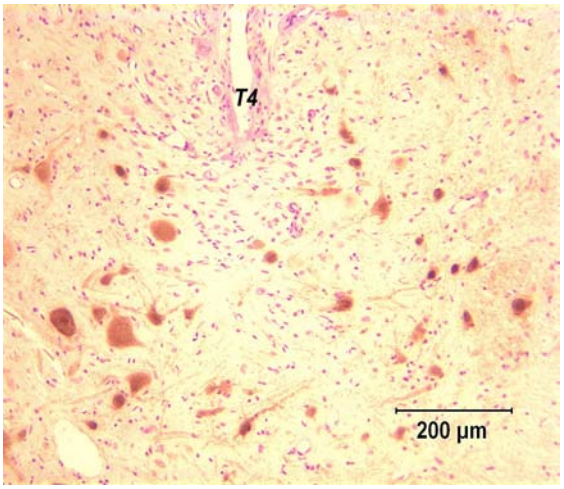

Figure 13B. Higher magnification of the tip site of shank T4. There is a reduction in the NeuN-positive neurons near the track, but viable neurons are seen within 100 ：m of the tip site, and there is minimal scarring around and ventral to the tip site. NeuN + Nissl counterstain.

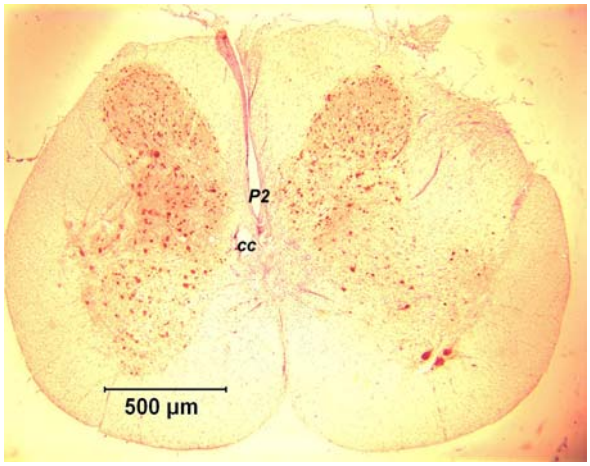

Figure 14. SP136. The track of stabilizing shank P2. The shank passed close to, or through, the central canal (cc). NeuN + Nissl counterstain

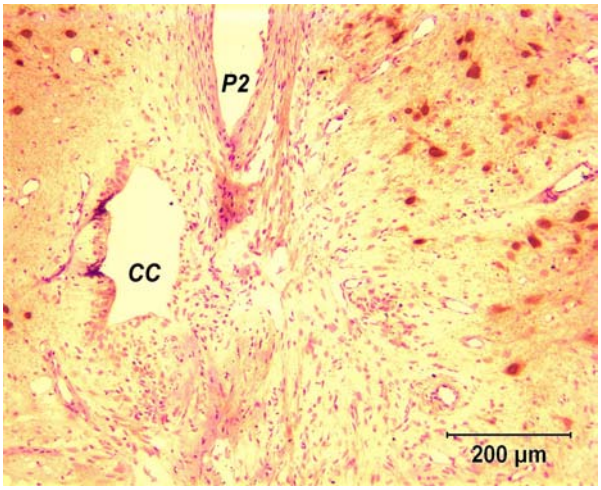

Figure 14B. Higher magnification of the region surrounding and ventral to shank 2. Note the extensive tissue damage and the damage to the ependema of the central canal (cc). Note the total absence of NeuN-positive neurons within the damaged region. NeuN + Nissl counterstain

REFERENCES

Nadelhaft, I., W. C. de Groat, and C. Morgan. Location and morphology of parasympathetic preganglionic neurons in the sacral spinal cord of the cat revealed by retrograde axonal transport of horseradish peroxidase. *J Comp Neurol* 193: 265-81., 1980.